Unconstrained Workloops Reveal Frequency-Phase Coupling in Compliant Muscle-Tendon Unit

Benjamin D. Robertson[1](bdrober3@ncsu.edu), Gregory S. Sawicki[1]

[1]Human PoWeR Lab, Joint Dept. of Biomedical Engineering at the University of North Carolina, Chapel Hill, NC and North Carolina State University, Raleigh, NC

Human PoWeR Lab

1 Introduction

- Despite joint and muscle redundancy, legs behave mechanically like a compliant spring **[1,2]**.
- Multiple muscle level studies of bouncing gait in humans **[3-7]** and animals **[2,8]** observe elastic 'tuning' in biological muscle-tendon units (MTU).
- While origins of elasticity in gait are clear, the role of neural control and environment in governing elastic behavior is not.
- The classical workloop technique has been used to investigate these questions. This approach imposes trajectories and varies phase of activation as a means of simulating functional mechanics **[9-10]**.
- In reality, limb trajectory is a consequence of active force generation, limb geometry, and inertial environment **[11].**
- We use a simulated inertial environment to explore how gravitational load, limb geometry, and frequency of muscle activation influence resonance tuning in a biological muscle-tendon unit (MTU) **[12-13]**.
- Linear systems theory predicts that driving an elastic system at its passive resonant frequency (ω_0) results in a peak response (i.e. force) accompanied by a phase shift in response centered at ω_0 **[14]**.
- We aimed to determine whether these control principles carry over to an actively driven/stiffened muscle-tendon unit of known passive resonant frequency.

2 Methods

Experimental Preparation: A schematic of experimental preparation used can be seen in **panel 3**. Plantaris muscle-tendon units from the American bullfrog Rana Catesbeiana were used in this study (n=6).

Procedure: For each muscle preparation 4 300 ms fixed end contractions were performed with varying amounts of passive tension to determine F_{max} (43.41 ±10.31 N), l_0(10.74 ± 2.89mm), v_{max}(-13.8$l_0 \cdot s^{-1}$, unpublished data), τ_{act} (0.066 ± 0.010 s) and τ_{deact} (0.100 ± 0.020 s) for each muscle used. In-silico environment inertial parameters (l_{in}, l_{out}, M, **panel 3**) were set assuming a passive MTU stiffness of 7,000 N/m to approximate a passive resonant frequency comparable to that of the human triceps surae-Achilles tendon complex ($\omega_0 \approx 2.2$ Hz) **[15]**. Following this, the inactive MTU was allowed to oscillate against our simulated inertial load to determine the actual system resonant frequency (ω_0= 2.34 ± .11 Hz).

Once ω_0 was determined, the biological MTU was driven at a range of frequencies about ω_0 ($\omega_{stim} = \pm 20\%\omega_0$in 10% increments) for 8 cycles with a stimulation duty of 10% to characterize the active system frequency response. The order of ω_{stim} conditions was randomized to counteract fatigue effects. The final 4 cycles from each condition were used in subsequent analysis.

Modeled Metabolic Cost: Dimensionless metabolic cost was modeled as a function of normalized instantaneous muscle velocity **[16]**, scaled by modeled active state and F_{max} **[17]**, and normalized to individual muscle mass (4.79 ± .98 g).

3 Muscle Prep.

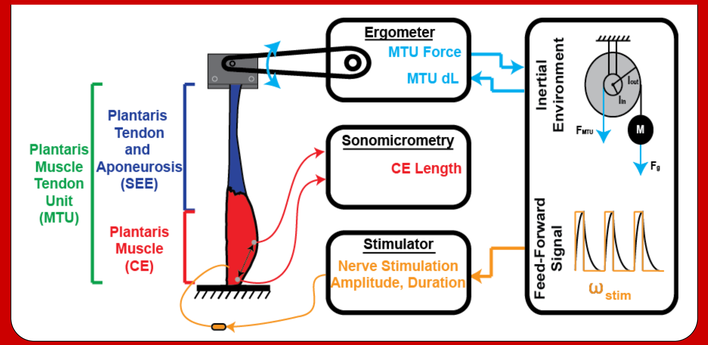

4 Hypotheses

(1) The biological MTU will reach a steady state (i.e. no net work over a stimulation cycle) at all driving frequencies.

Predictions from Linear Systems:
(2) Driving the biological MTU at ω_0 will maximize elastic energy storage and return in series elastic elements (i.e. tendon, aponeurosis).
(2) Driving the biological MTU at ω_0 will result in a peak response (i.e. MTU peak force).
(3) There will be a shift in the phasing of the system response centered at ω_0.

Energetic Predictions:
(4) Driving the biological system at ω_0 will result in minimal metabolic demand, and maximal MTU efficiency.

7 Results

Cycle Dynamics

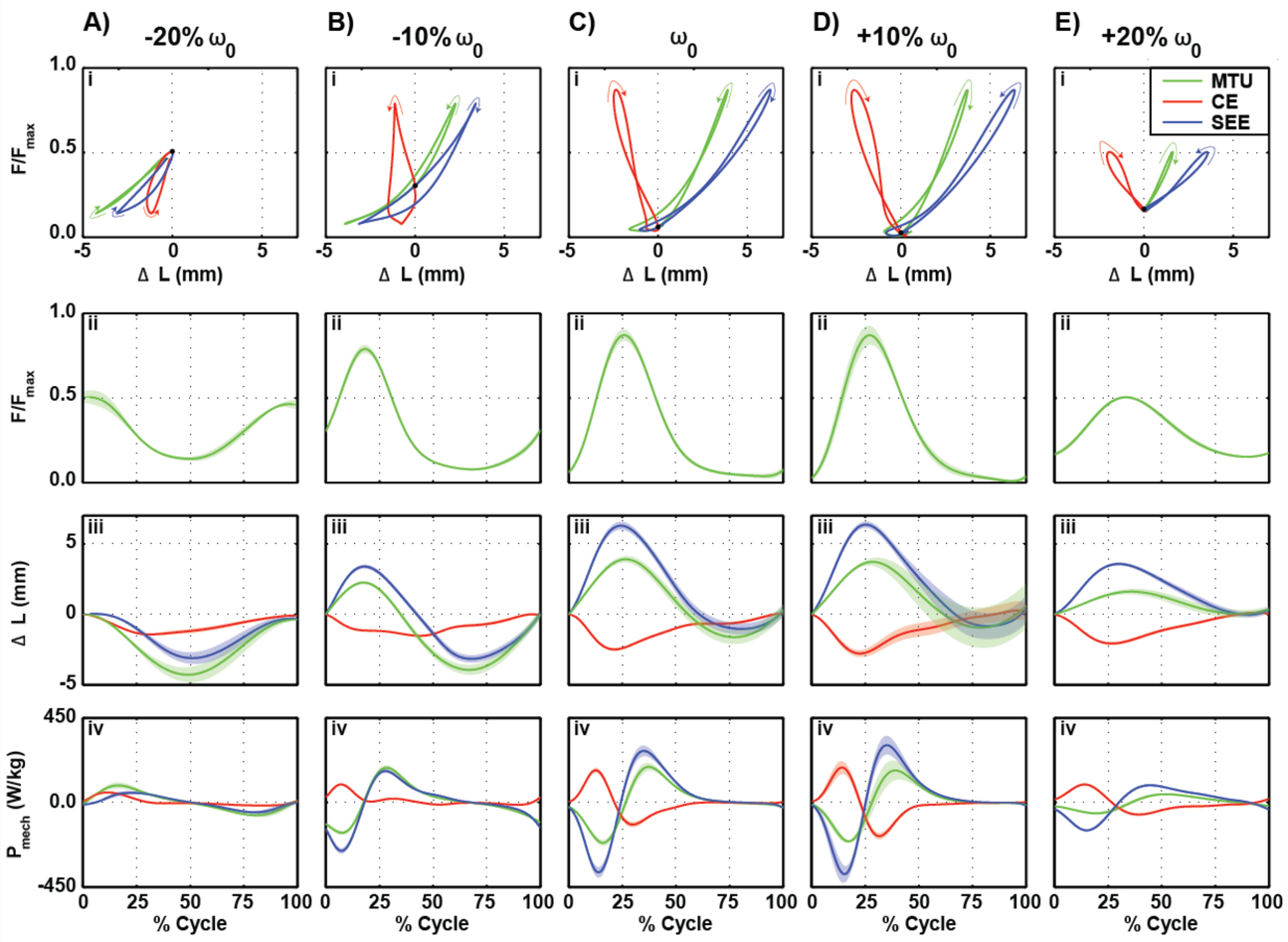

Figure 1: Mean dynamic behavior observed for a single subject at stimulation frequencies of **(A)** -20%ω_0, **(B)** -10%ω_0, **(C)** ω_0, **(D)** +10%ω_0, and **(E)** +20%ω_0. Plots of **(i)** Mean workloop behavior, **(ii)** Force ± 1SE vs. time, **(iii)** ΔL ± 1SE vs. time, and **(iv)** Power ±1SE vs. time are shown for each condition. Stimulation onset in all workloops **(i)** is indicated by a black dot. Margins of SE are indicated by opaque region surrounding mean behavior (solid line). Note that SE's are small, indicating generally periodic behavior.

Force Production Dynamics

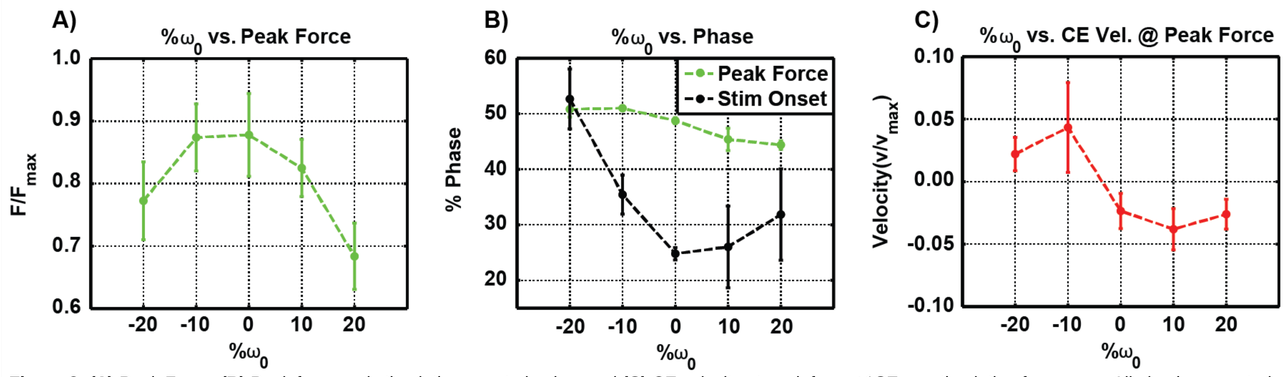

Figure 3: (A) Peak Force, **(B)** Peak force and stimulation onset phasing, and **(C)** CE velocity at peak force ±1SE vs. stimulation frequency. All phasing reported are relative to minimum MTU length from previous cycle of sitmulation **(B)**. Also note that v_{max} is a negative shortening velocity, i.e. a negative normalized velocity indicates lengthening at peak force

Modeled Metabolic Cost and Efficiency

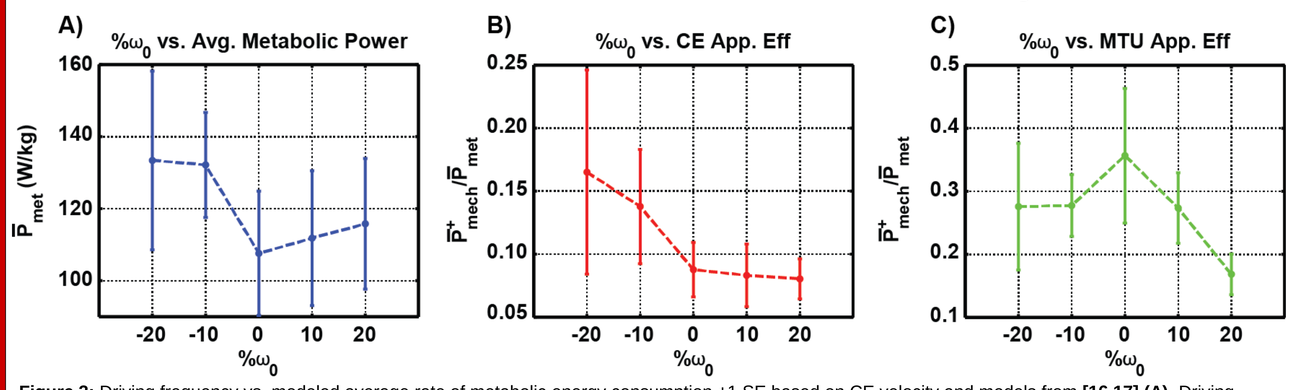

Figure 3: Driving frequency vs. modeled average rate of metabolic energy consumption ±1 SE based on CE velocity and models from **[16,17] (A)**. Driving frequency vs. average CE **(B)** and MTU **(C)** apparent efficiency ±1 SE. Note that a driving frequency of ω_0 is coincident with minimums in average metabolic power **(A)**, maximums in MTU apparent efficiency **(C)**, and relatively low CE efficiency **(B)**.

Power Output

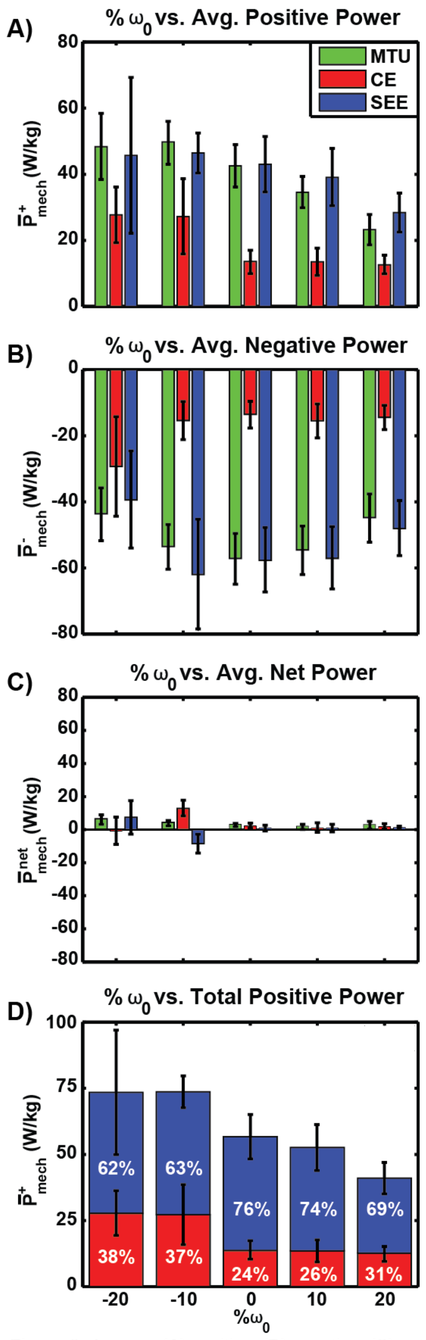

Figure 2: Average **(A)** positive, **(B)** negative, **(C)** net, and **(D)** total positive power ±1SE vs stimulation frequency. White numbers on bars in **(D)** indicate percent contribution from CE (red) and SEE (blue) to total average positive power over a stimulation cycle

8 Conclusions

(1) Steady state mechanics were achieved in all conditions, as evidenced by small variability in dynamics (**fig. 1**) and an average net work ~0 (**fig. 2c**).

(2) Maximal elastic energy storage and return was observed for driving frequencies of -10%ω_0 and ω_0. The greatest % contribution from SEE to overall power was observed at ω_0.

(3) The observed shift in system phasing is centered at a driving frequency <ω_0.

(4) Minimums in modeled metabolic demand and maximums in MTU apparent efficiency were coincident with a driving frequency of ω_0.

(5) Based on outcomes presented here, resonance in biological MTU may be a driving factor in preferred movement patterns.

9 Future Directions

Future work will modify the existing simulated environment to explore fundamental questions related to neuromechanical behavior and adaptation including:

- Modifying environment controllers to rapidly prototype and test exoskeletons for assisting compliant muscle-tendon units during bouncing gait.
- Perturb steady state behavior to explore the role that mechanical preflex plays in restoration of stability.
- Modify load characteristics and limb geometry to understand their role in augmenting compliant MTU behavior.

Work Cited

[1] Geyer, H et. al., *Proc. Biol. Sci.*, 2006.
[2] Roberts, T J, et al., *J Exp Biol.*, 2011.
[3] Dean, JC et. al. *J. Appl. Phys.*, 2011.
[4] Farris DJ et. al., *Proc. Natl. Acad. Sci.*, 2012.
[5]Grabowski et. al. *J. Appl. Physiol.*, 2009
[6] Takeshita et. al., *J. Appl. Physiol.*, 2006.
[7] Farris, Robertson, et. al., *J. Appl. Physiol.*, 2013.
[8]Biewener et. al., *Exerc. Sport Sci. Rev.*, 2000.
[9] Ettema, GJ et. al., *J. Exp. Biol.*, 1996.
[10] Barclay et. al., *J. Biomech.*, 2007.
[11] Marsh, RL. *J. Exp. Biol.*, 1999.
[12] Farahat, WA et. al., *PLoS Comp. Biol.*, 2010
[13] Clemente et. al., *Bioinspir. Biomim.*, 2012.
[14] Ogata, K., *Modern Control Engineering 4th ed.*, 2002.
[15] Robertson et. al., *J. Theor. Biol.*, 2014.
[16] Alexander, RM., *J. Theor Biol.*, 1997
[17] Krishnaswamy, P et. al., *PLoS Comp Biol.*, 2007.

Acknowledgements

We would like to thank Sid Vadakkeveedu for assistance during experiments, and the UNC/NCSU REC for a 25k pilot grant.